The Plant Cell, Vol. 14, 505–519, February 2002, www.plantcell.org © 2002 American Society of Plant Biologists

Characterization of Phenylpropene *O*-Methyltransferases from Sweet Basil: Facile Change of Substrate Specificity and Convergent Evolution within a Plant *O*-Methyltransferase Family

David R. Gang,[a,1,2] Noa Lavid,[b] Chloe Zubieta,[c] Feng Chen,[a] Till Beuerle,[a] Efraim Lewinsohn,[b] Joseph P. Noel,[c] and Eran Pichersky[a]

[a] Department of Molecular, Cellular and Developmental Biology, University of Michigan, Ann Arbor, Michigan 48109-1048
[b] Aromatic, Medicinal and Spice Crops Unit, Newe Ya'ar Research Center, Agricultural Research Organization, P.O. Box 1021, Ramat Yishay, 30095, Israel
[c] Structural Biology Laboratory, The Salk Institute for Biological Studies, 10010 North Torrey Pines Road, La Jolla, California 92037

Some basil varieties are able to convert the phenylpropenes chavicol and eugenol to methylchavicol and methyleugenol, respectively. Chavicol *O*-methyltransferase (CVOMT) and eugenol *O*-methyltransferase (EOMT) cDNAs were isolated from the sweet basil variety EMX-1 using a biochemical genomics approach. These cDNAs encode proteins that are 90% identical to each other and very similar to several isoflavone *O*-methyltransferases such as IOMT, which catalyzes the 4′-*O*-methylation of 2,7,4′-trihydroxyisoflavanone. On the other hand, CVOMT1 and EOMT1 are related only distantly to (iso)eugenol OMT from *Clarkia breweri*, indicating that the eugenol *O*-methylating enzymes in basil and *C. breweri* evolved independently. Transcripts for CVOMT1 and EOMT1 were highly expressed in the peltate glandular trichomes on the surface of the young basil leaves. The *CVOMT*1 and *EOMT*1 cDNAs were expressed in *Escherichia coli*, and active proteins were produced. CVOMT1 catalyzed the *O*-methylation of chavicol, and EOMT1 also catalyzed the *O*-methylation of chavicol with equal efficiency to that of CVOMT1, but it was much more efficient in *O*-methylating eugenol. Molecular modeling, based on the crystal structure of IOMT, suggested that a single amino acid difference was responsible for the difference in substrate discrimination between CVOMT1 and EOMT1. This prediction was confirmed by site-directed mutagenesis, in which the appropriate mutants of CVOMT1 (F260S) and EOMT1 (S261F) were produced that exhibited the opposite substrate preference relative to the respective native enzyme.

INTRODUCTION

The phenylpropenes are a group of small phenolic molecules, derived from the general phenylpropanoid pathway, that are key flavoring elements in many important herbs and spices, including peppercorns, cloves, nutmeg, cinnamon, allspice, pimenta, tarragon, and basil (Gildemeister and Hoffmann, 1913; Guenther, 1949; Lawrence, 1992). In addition, the phenylpropenes are important components of the defensive arsenal of plants or function as pollinator attractants. For example, eugenol is well documented to be an inhibitor of herbivory (Grossman, 1993; Sisk et al., 1996; Obeng-Ofori and Reichmuth, 1997) as well as a good nematocide (Chatterjee et al., 1982; Sangwan et al., 1990), fungicide (Karapinar and Aktug, 1987; Adams and Weidenborner, 1996), and bacteriocide (Miyao, 1975). In contrast, methyleugenol is an important insect pollinator attractant in many flowers, for pollinating moths and beetles in particular, and is a female pheromone mimic for several fruit flies (Shukla and Prasad, 1985).

Little is known about the biosynthesis of the phenylpropenes, such as eugenol, methyleugenol, and methylchavicol (Gang et al., 2001). Conflicting reports have left the question open of how the allyl/propenyl side chain of the phenylpropenes is formed (Manitto et al., 1974, 1975; Klischies et al., 1975; Senanayake et al., 1977). Other steps in the pathway, however, have been investigated further. Two *O*-methyltransferase (OMT) activities, operationally defined as eugenol OMT (EOMT) and chavicol OMT (CVOMT) (Figure 1A), identified in crude protein extracts of sweet basil, were able

[1] Current address: Department of Plant Sciences, University of Arizona, Tucson, Arizona 85721–0036.
[2] To whom correspondence should be addressed. E-mail gang@ag.arizona.edu; fax 520-621-7186.
Article, publication date, and citation information can be found at www.plantcell.org/cgi/doi/10.1105/tpc.010327.

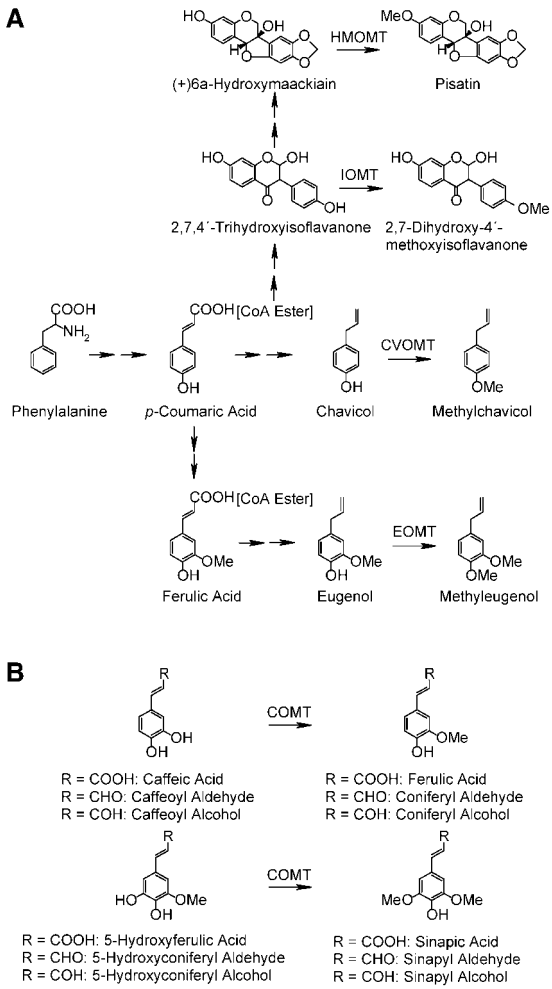

Figure 1. Role of Selected SMOMTs in Plant Specialized Metabolism.

(A) Simplified biochemical pathway leading to methylchavicol and methyleugenol in sweet basil and to the methoxylated isoflavonoids 2,7-dihydroxy-4′-methoxyisoflavanone and pisatin in legumes. Transformations catalyzed by CVOMT, EOMT, IOMT, and HMOMT are indicated by single arrows. Double arrows indicate multiple conversions.

(B) Selected conversions catalyzed by COMT.

to convert eugenol and chavicol, respectively, to methyleugenol and methylchavicol using *S*-adenosylmethionine (SAM) as the methyl donor (Wang, 1999; Lewinsohn et al., 2000; Gang et al., 2001). The ratio of these two activities was not constant between different protein extracts from the same basil line (Wang, 1999; D.R. Gang and E. Pichersky, unpublished data). Affinity purification of EOMT and CVOMT activities from basil leaves identified two polypeptides of similar molecular mass that could not be separated further (Wang, 1999). Furthermore, both of these activities appear to be restricted to the peltate glandular trichomes, the specialized structures on the surface of leaves and stems that are the site of synthesis and storage of the phenylpropenes in sweet basil (Gang et al., 2001). These results indicated that the methylation of eugenol and chavicol could be catalyzed by two separate but very similar enzymes or by a single polypeptide whose activity is modulated by some other factor to produce the observed differences in activities between extracts.

High-resolution SDS-PAGE indicated that the subunits of both EOMT and CVOMT have a molecular mass of ~40,000 kD, comparable to the size of other plant small molecule OMTs (SMOMTs) (Ibrahim et al., 1998; Wang, 1999). Enzymes belonging to this class include (iso)eugenol OMT (IEMT), which had been purified and cloned from *Clarkia breweri* (Wang and Pichersky, 1998). Antibodies to IEMT, an enzyme that evolved recently from caffeic acid/catechol OMT (COMT) in *C. breweri* (Wang and Pichersky, 1998), were able to cross-react with COMT from basil but not with the purified EOMT/CVOMT protein(s) (Wang, 1999), indicating that the latter probably were not evolved directly from COMT but could be more related to other plant SMOMTs.

Many other OMTs of the SMOMT class have been identified in plants. These enzymes play critical roles in the biosynthesis of many classes of compounds required for plant growth and plant defense. COMT itself, which catalyzes the *ortho*-methylation of aromatic diols (Figure 1B), may be involved in lignification (Ye and Varner, 1995; Maury et al., 1999; Guo et al., 2001; Parvathi et al., 2001) or may have other physiological functions (Collendavelloo et al., 1981; Pellegrini et al., 1993). Another group of SMOMTs is involved in the methylation of *para*-hydroxyl functionalities in the biosynthesis of small aromatic compounds in plants. Examples from this group include isoflavone OMT (IOMT; Figure 1A), which catalyzes the 4′-*O*-methylation of 2,7,4′-trihydroxyisoflavanone, and (+)-6a-hydroxymaackiain-3-OMT (HMOMT; Figure 1A), both of which are involved in the biosynthesis of phytoalexins in legumes (Wu et al., 1997; He et al., 1998). On the other hand, caffeoyl-CoA:SAM OMT (CCOMT), which catalyzes the *meta*-*O*-methylation of caffeoyl-CoA to form feruloyl-CoA and appears to play an important role in the formation of the coniferyl alcohol moieties that are precursors for lignification (Schmitt et al., 1991; Martz et al., 1998; Vander Mijnsbrugge et al., 2000), is not closely related in sequence to the SMOMT class that contains COMT, IEMT, IOMT, and HMOMT.

The three-dimensional crystal structures of IOMT and chalcone OMT (ChOMT), another protein belonging to the class of SMOMTs containing IOMT that is involved in the production of 4,4′-dihydroxy-2′-methoxychalcone, a *nod* gene inducer (Maxwell et al., 1992, 1993), were reported recently (Zubieta et al., 2001). The structures of these two enzymes are the first to be reported for their class of plant OMTs. This major breakthrough now makes it possible to determine the specific amino acid residues responsible for

conferring substrate specificity to this class of enzymes and thus to understand the structural differences that allow some enzymes, such as COMT, to have broad substrate specificities, whereas others, such as IOMT, have very narrow substrate specificities. Although the overall three-dimensional structures of the crystallized IOMT and ChOMT proteins are very similar, they have markedly different substrate preferences (i.e., their substrates, although similar in structure, are not interchangeable). This substrate discrimination is the result of two factors: first, shape selectivity was dictated by van der Waals interactions that were unique to each protein because of the specific complement and arrangement of aromatic and aliphatic side chains lining the active site binding pocket; second, efficient substrate binding was achieved by specific hydrogen bonding patterns (Zubieta et al., 2001). Thus, by the process of random mutations altering the amino acid residues surrounding the binding pocket, followed by selection, plants have evolved OMTs with distinct substrate preferences. This result provides a clear evolutionary mechanism whereby plants have been able to produce the great variety of specific enzymatic functions necessary for the production of the vast array of specialized metabolites (i.e., secondary metabolites) found in the plant kingdom.

To elucidate the biosynthetic pathway of the phenylpropenes in basil peltate glands, and specifically to characterize the OMT activities that convert chavicol to methylchavicol and eugenol to methyleugenol with respect to their structural properties and evolutionary origin, we recently produced an expressed sequence tag (EST) library from basil peltate glandular trichomes (Gang et al., 2001). In this library, we identified two types of OMTs that are very closely related to each other and that are related to IOMT. Here, we report that these ESTs represent transcripts for CVOMT and EOMT and that these enzymatic functions are encoded by separate genes that are closely related to each other and to IOMT and less related to IEMT and COMT. In addition, we show that CVOMT and EOMT are easily interconvertible via a single amino acid change, attesting to the relative ease by which such specific enzymatic activities can evolve in plants, thereby facilitating convergent evolution.

RESULTS

Isolation and Sequence Characterization of Basil CVOMT and EOMT cDNAs

We reported previously the construction of an EST database from peltate glandular trichomes isolated from the leaves of basil cv EMX-1 (Gang et al., 2001). A search in this database for potential OMTs revealed several cDNAs with varying degrees of similarity to known CCOMT sequences and one clone whose sequence was identical to a previously characterized COMT cDNA from basil (Wang et al., 1999). In addition, 19 ESTs (of 1250, or 1.5% of the total), representing two closely related types of sequences, showed the highest similarity to IOMT (among OMTs whose function is known). Because all of these 19 ESTs (18 of one type, one of the other type) were found to be incomplete, 5′ rapid amplification of cDNA ends (Chenchik et al., 1996; Matz et al., 1999) followed by reverse transcriptase–mediated polymerase chain reaction (RT-PCR) was used to obtain full-length cDNAs, and genome walking (Siebert et al., 1995) verified that the rapid amplification of cDNA ends products were complete and accurate.

The two types of complete cDNAs, designated EOMT1 and CVOMT1 based on the data presented below, were found to be 90% identical to each other at the protein level. Their evolutionary relationships to a large family of plant OMTs (SMOMTs, also designated in the literature as the

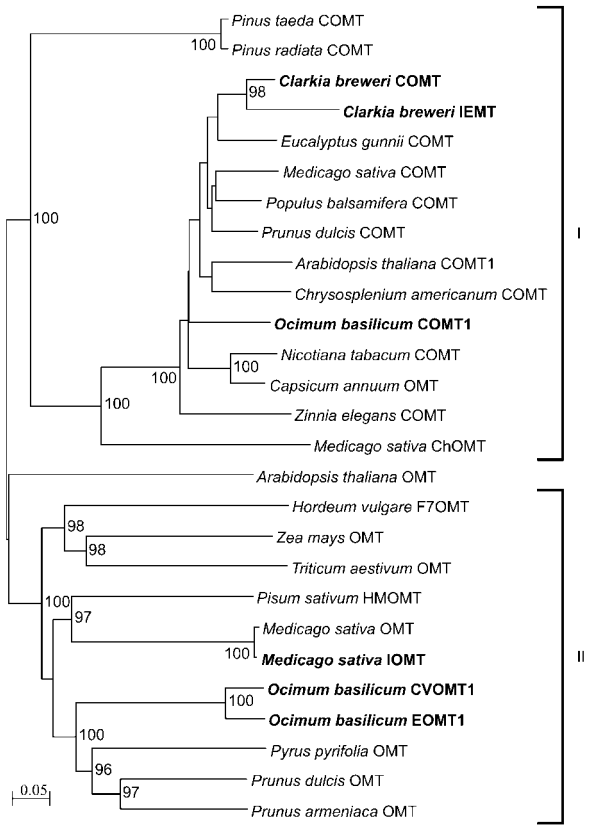

Figure 2. Members of the COMT Superfamily of Plant SMOMTs Fit into Two Classes Based on Sequence Homology.

Class I contains COMTs and enzymes such as *C. breweri* IEMT, which evolved recently from this class. Class II contains OMTs that use a variety of substrate structures. *Arabidopsis thaliana* OMT does not fit into either class. The sequences of the genes with names in boldface are compared in Figure 3.

COMT superfamily) that catalyze the formation of some specialized, or secondary, metabolites are illustrated in Figure 2. This family includes genes for COMT, IOMT, HMOMT, and ChOMT as well as a number of related genes with no known function, for example, putative OMTs from several species in the rose family (*Pyrus* and *Prunus* species) (Mbeguie-A-Mbeguie et al., 1997; Suelves and Puigdomenech, 1998). In the evolutionary tree presented in Figure 2, there is a clear division between all known COMT sequences with the *C. breweri* IEMT on one side and the flavone and isoflavone OMTs plus the basil EOMT1 and CVOMT1 on the other side.

From examination of the crystal structure of IOMT, His-257 of IOMT was implicated as the residue responsible for the deprotonation of the aromatic hydroxyl group of the substrate, which initiates the Sn2 attack on the methyl group of SAM (Zubieta et al., 2001). Asp-288 and Glu-318 were shown to constrain the basic His-257, both sterically and by hydrogen bonding, thereby facilitating efficient catalysis. These amino acid residues are conserved in CVOMT1

```
CbrCOMT    MGSTGNAETQLTPTHVSDEEAN-LFAMQLASASVLPMVLKAAIELDVLEIMAKSIPHGSGAYISPAEIAAQLPTTN 75
CbrIEMT    MGSTGNAEIQIIPTHSSDEEAN-LFAMQLASAAVLPMALKAAIELDVLEIMAKSVPP--SGYISPAEIAAQLPTTN 73
ObaCOMT1   MGSATN-----TPQINSDEEENFLFAMQLASASVLPMVLKSAIELDLLELIKKSGAG---AFVSPVDLAAQLPTTN 68
ObaEOMT1    MALQKVDISLSTEQLLQAQVH--VWNHMY-AFANSMSLKCAIQLGIPDILHKHGRP-----MTLSQLLQSIPINK 67
ObaCVOMT1   MALQNMDISLSTEQLLQAQAH--VWNHMY-AFANSMSLKCAIQLGIPDILHKHDRP-----MTLSQLLKAIPINK 67
MsaIOMT     MASSINGRKPS--EIFKAQA--LLYKHIY-AFIDSMSLKWAVGMNIPNIIHNHGKP-----ISLSNLVSILQVPS 65
                 *              *                    ▼ ▼▼          *              **

                                                                          iii
CbrCOMT    PDAPVMLDRVLRLLASYSVVTCSLRELPDGKVERLYGLAPVCKFLTKNEDGVSLAPLCLMNQDKVLMESWYYLKDA 151
CbrIEMT    PEAPVMLDRVLRLLASYSVVTYTLRELPSGKVERLYGLAPVCKFLTKNEDGVSLAPFLLTATDKVLLEPWFYLKDA 149
ObaCOMT1   PDAHVMLDRILRLLTSYAILECRLKTLPDGGVERLYGLAPVCKFLTKNEDGVSMAPLTLMNQDKVLMESWYHLSDA 144
ObaEOMT1   EKTQCFQRLMRALVNSNFFIEENN----FNNQEVCYWLTPASCLLLKEAP-LTVAPLVQVVLDPTFTNPWHHMSEW 138
ObaCVOMT1  EKSQSFQRLMRALVNSNFFIEEN-----SNNQEVCYWLTPASRLLLKGAP-LTVAPLVQVVLDPTFTNPWHYMSEW 137
MsaIOMT    SKIGNVRRLMRYLAHNGFFEIIT-------KEEESYALTVASELLVRGSD-LCLAPMVECVLDPTLSGSYHELKKW 133
             * *                  *    *            *    *           ▲▲    ▲▲  ▲ *

                                                                  --Box I--
CbrCOMT    ILDG--GIPFNKAYGMTAFEYHGTDPRFNKVFNRGMSDHSTITMKKIFEMYTG-FEALNTIVDVGGGTGAVLSMIV 224
CbrIEMT    ILEG--GIPFNKAYGMNEFDYHGTDHRFNKVFNKGMSSNSTITMKKILEMYNG-FEGLTTIVDVGGGTGAVASMIV 222
ObaCOMT1   VVDG--GIPFNKAYGMTAFEYHGTDPRFNKVFNQGMSNHSTITMKKILETYTG-FDGLKTVVDVGGGTGATLNMIV 217
ObaEOMT1   FTHEKHATQFEAANGCTFWEKLANEPSKGRFFDEAMSCDSRLVAHVFTKDYKHVIEGIRTLVDVGGGNGTMAKAIV 214
ObaCVOMT1  FKHENHATQFEAANGCTFWEKLANKPSMGRFFDEAMSCDSRLVAHVLTKDYKHVIDGIRTLVDVGGGNGTMAKAIV 213
MsaIOMT    I-YEEDLTLFGVTLGSGFWDFLDKNPEYNTSFNDAMASDSKLI-NLALRDCDFVFDGLESIVDVGGGTGTTAKIIC 207
             *  *    ▲       ▲      *  *   ▲   ▲          *       *      § §

                --Box II-          -Box III-                                    --Box
CbrCOMT    AKYPSIKGINFDLPHVIEDAPIYPGVEHVGGDMFVSVPKGDAIFMKWICHDWSDEHCLKFLKNCYAALPEHG---K 297
CbrIEMT    AKYPSINAINFDLPHVIQDAPAFSGVEHLGGDMFDGVPKGDAIFIKWICHDWSDEHCLKLLKNCYAALPDHG---K 295
ObaCOMT1   SKYPSIKGINFDLPHVIEDAPSYPGVEHVGGDMFVSVPKGDAIFMKWICHDWSDEHCVKFLKNCYDALPQNG---K 290
ObaEOMT1   EAVPTIKCTVIDLPHVVAGLESTDNLNYIGGDMFQSIPSADAILLKSIIHDWDDVEGLKILKKCKDTVVMEG---K 287
ObaCVOMT1  EAVPTMKCTVLDLPHVVAGLESTGKLSYIGGDMFQSIPSADAILLKFIIHDWDDEEGLKILKRCKDAVGIGG---K 286
MsaIOMT    ETFPKLKCIVFDRPQVVENLSGSNNLTYVGGDMFTSIPNADAVLLKYILHNWTDKDCLRILKKCKDAVTNDGKRGK 283
                *    *§§          ** *    §§            §*  ©^§  *       *     ***

           IV-                            -Box V-
CbrCOMT    VIVAECILPLSPDPSLATKGVIHIDAIMLAHNPGGKERTEKEFEALAIGAGFKGFKVACCAFNTYVMEFLKTA 370
CbrIEMT    VIVAEYILPPSPDPSIATKVVIHTDALMLAYNPGGKERTEKEFQALAMASGFRGFKVASCAFNTYVMEFLKTA 368
ObaCOMT1   VILAECVLPEAPDTGLATKNVVHIDVIMLAHNPGGKERTEKEFQGLAKAAGFKQFNKACCAYNTWIMELLK   361
ObaEOMT1   VIIIDVVVGVNHDIDEVLEDQLHFDMAMMCYFN-AKERTMSEWEKLIYNAGFKSYKLTPAFGVRSLIEAYP   357
ObaCVOMT1  VIIIDVVVGVNHDIDEVLEDQLHFDMAMMCYFN-AKERTMNEWEKLISAAGFTSYKLTPAFGVRSLIEAYP   356
MsaIOMT    VTIIDMVINEKKDENQVTQIKLLMDVNMAC—LN-GKERNEEEWKKLFIEAGFQHYKISPLTGFLSLIEIYP   352
              ©                  ▲  ▲▲ ▲ ▲    ©   *      **    *
```

Figure 3. Amino Acid Sequence Alignment Comparing Selected Members of the COMT Superfamily of Plant OMTs.

CbrCOMT, *C. breweri* COMT; CbrIEMT, *C. breweri* IEMT; ObaCOMT1, sweet basil COMT1; ObaEOMT1, sweet basil EOMT1; ObaCVOMT1, sweet basil CVOMT1; MsaIOMT, alfalfa IOMT. Box I through box V domains are conserved among plant SMOMTs. §, SAM binding; ©, catalytic residue; *, difference between EOMT and CVOMT; ^, binding pocket residue for CVOMT; ▲, substrate binding (from IOMT structure); ▼, substrate binding on other dyad polypeptide active site; i, residues important for the difference in activity between CbrCOMT and CbrIEMT.

and EOMT1 (Figure 3), suggesting that they are the catalytic residues in these enzymes as well. In addition, several consensus sequences were described previously as being signature motifs of the plant SMOMT group of enzymes (Ibrahim et al., 1998). Based on the crystal structure of IOMT (Zubieta et al., 2001), these motifs, also found in CVOMT1 and EOMT1 sequences (boxes I to V in Figure 3), play important roles in SAM binding (boxes I, II, and III) and catalysis (box V). Box IV was thought to play a role in metal binding and to help to orient Asp-288 properly in the active site (Ibrahim et al., 1998), but no bound metal was found in the structures of IOMT and ChOMT (Zubieta et al., 2001), so the actual function of this conserved region is not clear. Other residues implicated from the structure of IOMT as forming part of the substrate binding pocket also are conserved in EOMT1 and CVOMT1 (Figure 3).

Tissue-Specific Expression of Basil *CVOMT*1 and *EOMT*1 Genes and Tissue-Specific CVOMT and EOMT Enzymatic Activities

To determine the tissue in which *EOMT*1 and *CVOMT*1 are expressed, total RNA was purified from peltate glandular trichomes isolated from young developing leaves (<1.0 cm long) of basil lines EMX-1 and SW as well as from whole leaves of the same size grown under identical conditions. These RNA preparations were used in RNA gel blot analysis to detect and quantitate *EOMT*1 and *CVOMT*1 mRNAs. The EMX-1 basil line produces phenylpropenes that are methylated at the para position (methylchavicol and some methyleugenol), and the SW basil line produces the phenylpropene eugenol that is not methylated at the para position (Gang et al., 2001). Because of the high sequence similarity between *CVOMT*1 and *EOMT*1, a single phenylpropene OMT probe was used for all RNA gel blot analysis, and the signal detected in these experiments was the sum of the two types of transcripts. As can be seen in Figure 4A, lane 2, basil line EMX-1 peltate glands express these genes at much higher levels than whole leaf tissue (lane 1), whereas transcripts for *EOMT*1 and *CVOMT*1 are lacking in the SW line (lanes 3 and 4). These results verified previous assays that indicated that active EOMT1 and CVOMT1 enzymes were restricted to the peltate glands (Gang et al., 2001) of basil varieties that produce *para*-*O*-methylated phenylpropenes.

Further experiments were performed to determine how *EOMT*1/*CVOMT*1 gene expression and activity were regulated developmentally in basil line EMX-1. Leaves of three sizes—0.5, 1, and 3 cm long—were collected and analyzed (as a whole) for transcript levels and for specific enzymatic activities. Total RNA was isolated and hybridized with the basil phenylpropene OMT probe. As can be seen in Figure 4A, lanes 5 to 7, respectively, the basil OMTs were expressed at much higher levels in 0.5- and 1-cm leaves than in 3-cm leaves. EOMT and CVOMT enzyme activities (Figure 4B, lanes 5 to 7) also were much higher in very young developing leaves (0.5 cm) than in older, more developed leaves.

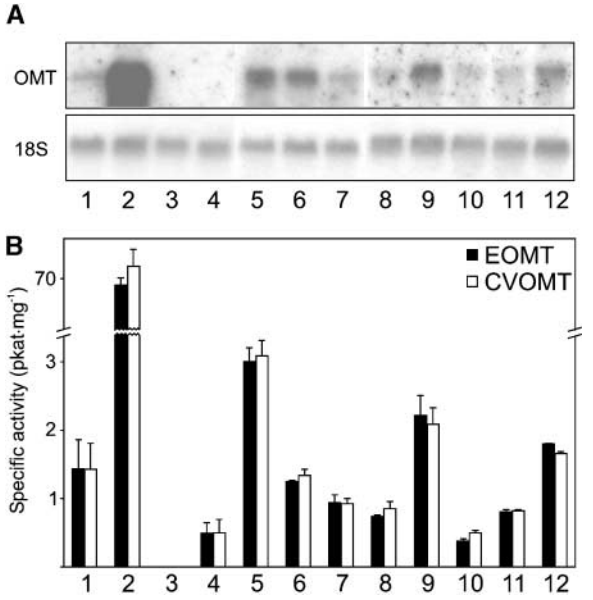

Figure 4. Tissue-Specific Expression of Basil Phenylpropene OMTs.

(A) RNA gel blot analysis of gene expression. Lanes 1 to 4 (3 μg of total RNA per lane) show comparison of gene expression in whole leaves (lanes 1 and 3) and in isolated peltate glandular trichomes (lanes 2 and 4) from basil lines EMX-1 (lanes 1 and 2; produces *para*-*O*-methylated phenylpropenes) and SW (lanes 3 and 4; produces non-*para*-*O*-methylated phenylpropenes). Lanes 5 to 7 (5 μg of total RNA per lane) show comparison of gene expression between different stages of leaf development from EMX-1 whole leaves 0.5 cm long (lane 5), 1 cm long (lane 6), and 3 cm long (lane 7). Lanes 8 to 12 (5 μg of total RNA per lane) show comparison of gene expression in different parts of EMX-1 leaves: lane 8, 1-cm leaf apical half; lane 9, 1-cm leaf basal half; lane 10, 3-cm leaf apical third; lane 11, 3-cm leaf middle third; lane 12, 3-cm leaf basal third.

(B) Specific activities for EOMT (black bars) and CVOMT (white bars) enzymes. Lane numbers indicate tissues as described for **(A)**. Bars indicate ±SE.

To further localize the site of EOMT and CVOMT enzymatic activities and mRNAs in older leaves, 1- and 3-cm leaves were cut perpendicularly to the midvein into halves and thirds, respectively, and analyzed for basil OMT expression and enzyme activity. As can be seen in Figure 4A, lanes 8 to 12, the OMT transcripts are expressed at much higher levels in the basal portion of the leaf (in both 1- and 3-cm leaves), which is still undergoing cell division and expansion, than in the leaf tip, which has ceased most growth processes. Enzymatic assays (Figure 4B, lanes 8 to 12) supported this observation as well. In all tissue samples examined, the amount of EOMT activity was approximately equivalent to CVOMT activity (Figure 4B).

Because our RNA gel blot experiments did not distinguish between *EOMT*1 and *CVOMT*1 transcripts, we used a quantitative RT-PCR procedure (see Methods) to determine what proportion of transcripts observed in the RNA gel blots were *CVOMT*1 transcripts and what proportion were *EOMT*1 transcripts. In leaves of various stages of development, as well as in isolated peltate glands, *CVOMT*1 accounted for ~90 to 95% of the total transcripts, whereas *EOMT*1 accounted for the rest (data not shown). The ratio of *CVOMT*1 to *EOMT*1 transcripts, together with the observation that EOMT catalytic efficiency with eugenol is ~10-fold higher than CVOMT catalytic efficiency with chavicol (see below), explain why the levels of EOMT activity in the tissues examined were approximately equivalent to CVOMT activity levels.

Enzyme Activities of Recombinant Proteins

The coding regions of *CVOMT*1 and *EOMT*1 were transferred to the expression vector pCRT7/CT-TOPO TA (Invitrogen, Carlsbad, CA) for functional expression as nonfusion proteins. COMT1 from basil (Wang et al., 1999), expressed from the pET28 vector, also was characterized.

All three OMT proteins (CVOMT1, EOMT1, and COMT1) were purified to 70 to 95% homogeneity using gel filtration and ion exchange chromatographic separations. Purified enzyme for each recombinant protein was used for the determination of general catalytic properties and kinetic parameters and the determination of substrate specificity (Table 1). All three proteins displayed in SDS-PAGE a subunit molecular mass of ~40,000 D (data not shown), which is very comparable to the values calculated from the translated amino acid sequences of the corresponding genes. This also is the size obtained for the CVOMT/EOMT mixture that was purified previously from basil leaf extracts (Wang, 1999). However, all three recombinant proteins eluted from a calibrated gel filtration column as 81,000- to 87,000-D proteins (EOMT eluted as slightly smaller than CVOMT and COMT), suggesting that all three proteins exist as homodimers in solution. This is not surprising, because other members of this family of OMTs, including the recently crystallized IOMT and ChOMT, also exist in solution as homodimers (Zubieta et al., 2001).

The expressed recombinant proteins all possessed a pH optimum from 7 to 8. In addition, increasing concentrations of salt (NaCl) >50 mM (or ammonium sulfate of comparable ionic strength) reduced enzymatic activity linearly with salt concentration. No difference in activity was observed for the enzymes from 0 to 50 mM NaCl. All three enzymes appeared to be catalytically stable at temperatures up to ~30°C. Assays with crude basil leaf extracts for EOMT, CVOMT, and COMT activities also displayed the same pH optima and temperature dependence, indicating that the recombinant proteins behaved similarly, if not identically, to the native enzymes.

All three enzymes (CVOMT1, EOMT1, and COMT1) were evaluated under standard conditions for their ability to catalyze the SAM-dependent *O*-methylation of a large number of potential substrates. The results of these assays, as well as a representative sampling of the compounds tested, are illustrated in Figure 5. As can be seen, CVOMT1 is the most specific of the enzymes in terms of substrate preference, and it catalyzes the *O*-methylation of chavicol much more readily than it does any other compound tested. Other compounds with a *para*-hydroxyl functional group, such as eugenol, *t*-isoeugenol, *t*-anol, caffeic acid, and phenol, served as poorer substrates. EOMT1, on the other hand, was found to methylate eugenol most efficiently, with *t*-isoeugenol and chavicol being poorer substrates. Interestingly, the substrate preference of EOMT1 differed from that of *C. breweri* IEMT (Wang and Pichersky, 1998, 1999), which instead uses *t*-isoeugenol and eugenol almost equally well as substrates, although the former was a slightly better substrate. Chavicol also was a poorer substrate for EOMT1 than it was for IEMT. Thus, EOMT1 from basil is more specific in its substrate preference than IEMT from *C. breweri*.

CVOMT1 and EOMT1 discriminated against potential substrates that did not have an allylic side chain in the *para* position relative to the hydroxyl group that was methylated. Thus, chavicol, but not *t*-anol, served as a good substrate for CVOMT1, and eugenol served as a better substrate for EOMT1 than did *t*-isoeugenol. *t*-Anol and *t*-isoeugenol possess propenyl and not allylic side chains (Figure 5). In addi-

Table 1. Properties of Basil Phenylpropanoid OMTs

Enzyme	Holoenzyme Mass (D) by Gel Filtration	Subunit Mass (D) by SDS-PAGE	Calculated Subunit Mass (D)	pH Optimum	Apparent K_m (μM) for SAM	Substrate	Apparent K_m (μM) for Substrate	Apparent V_{max} (pkat·mg^{-1})	k_{cat} (s^{-1})	k_{cat}/K_m (nM^{-1}·s^{-1})
COMT1	87,000	~40,000	39,529	7 to 8	64	Caffeic acid	47	19,500	1.3×10^{-2}	0.27
						Catechol	290	6900	4.6×10^{-3}	0.02
EOMT1	81,000	~40,000	40,237	7 to 8	5	Eugenol	3	4600	3.1×10^{-3}	1.23
						t-Isoeugenol	10	1900	1.3×10^{-3}	0.13
						Chavicol	7	1300	8.7×10^{-4}	0.13
CVOMT1	87,000	~40,000	39,937	7 to 8	5	Chavicol	6	1200	8.0×10^{-4}	0.13

tion, compounds with hydrophilic functionalities on the end of the alkene side chain (e.g., coniferyl alcohol, ferulic acid, and *p*-coumaric acid) were poor substrates for both CVOMT1 and EOMT1.

Basil COMT1 displayed a broad substrate preference, using a number of aromatic diols as substrates. *Ortho*-diols (e.g., catecol) were much better substrates than were *meta*- or *para*-diols (e.g., resorcinol and hydroquinone, respectively). Although CVOMT1 and EOMT1 preferred substrates with very hydrophobic side chains, COMT1 preferred substrates with either no alkene side chain (e.g., catecol) or with hydrophilic functionalities on the end of the side chain (e.g., caffeic acid). However, the aromatic hydroxyl group that becomes methylated by COMT1 resides at the position *meta* to the alkyl side chain (if such a side chain is present in the substrate). Thus, caffeic acid, which possesses a hydroxyl group *meta* to the side chain, is methylated, whereas *p*-coumaric acid, whose hydroxyl group is in the *para* position, is not a substrate for COMT1.

Kinetic parameters for each enzyme also were determined. These are listed in Table 1. The kinetic parameters for both EOMT1 and CVOMT1 with regard to chavicol as a substrate were identical, especially the apparent catalytic efficiency (k_{cat}/K_m ratio) and the absolute values for apparent V_{max} and apparent K_m. This finding indicates that both enzymes treat chavicol identically as a substrate (see legend to Figure 5). In addition, for EOMT1, the apparent catalytic efficiency for chavicol and *t*-isoeugenol was identical and ~10-fold lower than that for eugenol, again supporting eugenol as the favored substrate. However, the apparent K_m for *t*-isoeugenol was approximately twofold higher than the apparent K_m for chavicol, confirming the observation that binding of an allylic, and not a propenyl, side chain is favored by EOMT1. The apparent catalytic efficiency of *t*-isoeugenol *O*-methylation was the same as for chavicol because of the increase in apparent V_{max}, presumably attributable to the methoxyl group at the end of the substrate, which would be able to form hydrogen bonds to stabilize the binding of the transition state at that end of the molecule once it had bound. EOMT1 and CVOMT1 reacted in a like manner toward the cofactor SAM, with an apparent K_m for this substrate at 5 μM for both enzymes.

The only apparent catalytic difference between EOMT1 and CVOMT1 is that CVOMT1 has a very restricted substrate preference (see above), whereas EOMT1 can use eugenol and *t*-isoeugenol much more effectively as substrates (with much higher apparent V_{max} and higher apparent k_{cat}/K_m ratio).

COMT1 had much higher K_m values (10-fold higher) for SAM and its substrates than did EOMT1 and CVOMT1 (Table 1), supporting the notion that it is a less specific enzyme. However, COMT1 is able to achieve a catalytic efficiency toward its substrates that is similar to the apparent catalytic efficiency (k_{cat}/K_m) of EOMT1 toward its substrates, because COMT1 displays a much higher apparent V_{max}. In addition, COMT1 did not appear to display the dramatic substrate inhibition that was observed for CVOMT1 and EOMT1.

Relative Activity (%) for Each Enzyme Assayed

Substrate	CVOMT1	EOMT1	COMT1
Chavicol	100.0	24.0	2.7
Eugenol	4.0	100.0	8.1
t-Isoeugenol	3.4	26.0	3.9
Guaiacol	0.0	29.9	0.0
t-Anol	5.7	0.0	2.2
Caffeic Acid	0.0	2.3	100.0
Catechol	0.5	0.0	96.1
Pyrogallol	0.0	0.0	88.9
Protocatechuic Aldehyde	0.0	0.0	69.4
Resorcinol	0.0	0.0	10.4
Phenol	10.9	0.0	2.6
Coniferyl Alcohol	0.4	1.2	2.3
Ferulic Acid	0.0	0.7	2.2

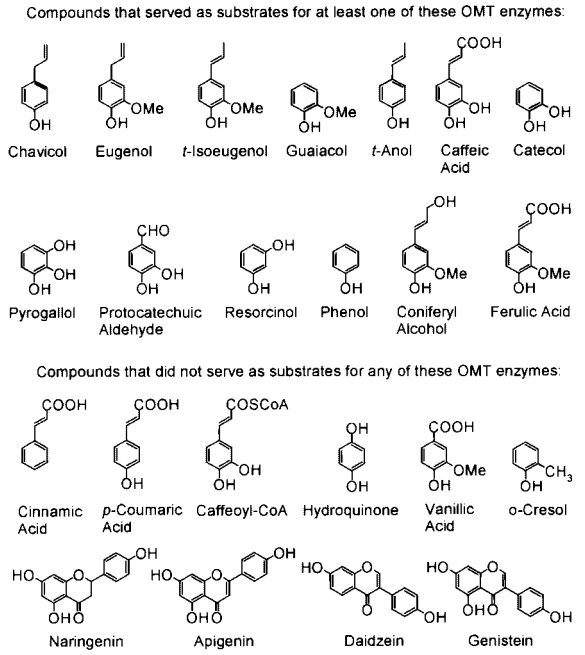

Figure 5. Comparison of Relative Specific Activities of Basil CVOMT1, EOMT1, and COMT1 with a Variety of Substrates.

For each enzyme, the specific activity that is the highest is set at 100%; although EOMT has similar activity with chavicol as CVOMT, its activity with eugenol is fourfold higher.

Modeling of Basil EOMT and CVOMT Active Sites

Basil CVOMT1 and EOMT1 tertiary and quaternary structures were modeled based on the recently published crystal structures of IOMT from alfalfa (Zubieta et al., 2001). These models supported the observation that these two enzymes

exist in solution as dimers, with a small N-terminal domain involved in dimerization, as was observed for IOMT (Zubieta et al., 2001). Based on the molecular modeling data, EOMT1 appears to form a more compact homodimer than CVOMT1, which appears to be more extended. This would explain the slightly different behavior of EOMT1 on the gel filtration column (eluting as an 81,000-D protein instead of 87,000 D, as CVOMT1 does).

Interestingly, the active sites of CVOMT1 and EOMT1 (Figures 6A and 6B, respectively) are almost identical. The substrate binding pockets of both enzymes are lined with the same aromatic and aliphatic amino acid side chains (with one exception; see below), producing a very hydrophobic environment for substrate binding. The substrates chavicol and eugenol also were modeled into the active sites of their respective enzymes. Based on this modeling, several amino acid residues were implicated in catalysis.

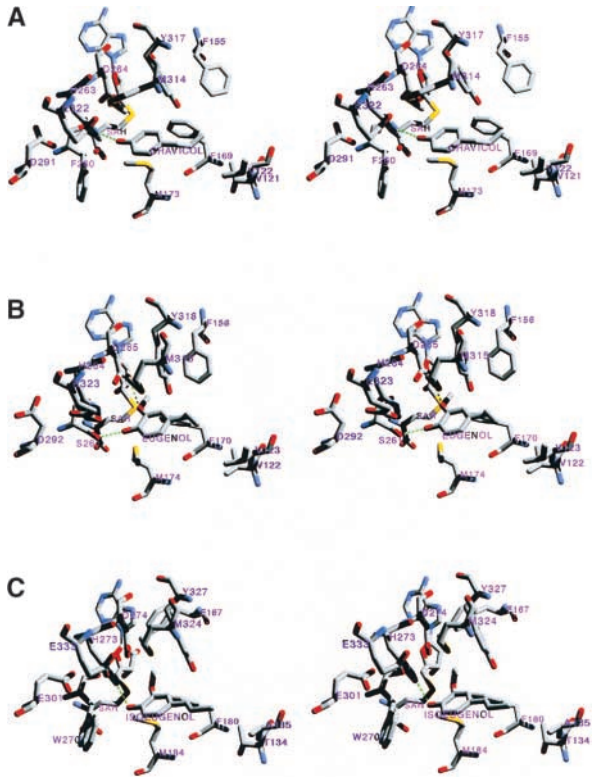

Figure 6. Stereo Views of the Three-Dimensional Structures of the Active Sites of Basil CVOMT **(A)**, Basil EOMT **(B)**, and *C. breweri* IEMT **(C)** as Determined by Molecular Modeling Based on the Crystal Structure of Alfalfa IOMT.

The most efficient phenylpropene substrate for each enzyme is shown bound, as is *S*-adenosylhomocysteine (the cofactor product), which was cocrystalized with IOMT to produce the original three-dimensional structure.

These include Ser-261, His-264, Asp-265, and Glu-323 for EOMT1 and His-263, Asp-264, and Glu-322 for CVOMT1. The amino acid residue numbers are off by one between the two enzymes as a result of the presence of Asn-91 in EOMT1, which is lacking in CVOMT1. Asn-91 resides in an external loop region of the protein that is far removed from the active site and appears to play no role in catalysis.

Based on these models, one major difference was observed between the active sites of EOMT1 and CVOMT1. In EOMT1, Ser-261 appears to play a critical role in forming a hydrogen bond with the *para*-hydroxyl group of the substrate eugenol, stabilizing the binding of the substrate in the active site. His-264 appears to interact with Ser-261 in this process. In addition, His-264 appears to be the catalytic residue, responsible for initiating the deprotonation of the hydroxyl group to form the reactive substrate intermediate that attacks the electrophilic methyl group of the SAM cofactor in the nucleophilic addition of the methyl group to the substrate. Asp-265 appears to form a hydrogen bond with the methoxyl oxygen of the eugenol substrate, further stabilizing substrate binding. Glu-323, which also is near His-264 in the active site, can form a hydrogen bond to the imidazole ring of His-264, apparently stabilizing the catalytic process. Thus, the interactions between His-264, Asp-265, Glu-323, and Ser-261 with each other and with the substrate appear to be critical for efficient catalytic function.

In CVOMT1, however, position 260 contains a phenylalanine residue instead of serine. Phe-260 is not able to form the hydrogen bond necessary to stabilize the binding of the substrate. Instead, this stabilization must be performed by His-263 alone. In addition, the larger phenyl ring of Phe-260 causes a shift in the orientation of His-263, which must be stabilized by a shift in the orientation of Glu-322. The alteration in the position of His-263 also causes a shift in the orientation of the bound substrate, making hydrogen bonds to Asp-264 less favorable. Thus, substrates such as eugenol and *t*-isoeugenol are less likely to be stabilized in the active site. Chavicol, which is smaller and does not possess the *meta* aromatic methoxyl functional group, still is able to bind.

In addition to the modeling of CVOMT1 and EOMT1, we modeled the *C. breweri* IEMT three-dimensional structure (Figure 6C), based on the IOMT structure, and found that its active site was very similar to the active site of EOMT1 and CVOMT1. Again, His-273, Asp-274, and Glu-333 appear to be involved in catalysis and substrate binding, but the serine found at position 261 of EOMT1 is a tryptophan (Trp-270) in IEMT. This causes lower binding affinity for the substrate (a 10-fold increase in apparent K_m compared with EOMT1 [Wang and Pichersky, 1999]). Unlike CVOMT1, however, IEMT does not appear to display substrate inhibition, so its apparent catalytic efficiency toward *t*-isoeugenol (Wang and Pichersky, 1999) is very similar to the apparent catalytic efficiency of EOMT1 toward eugenol (because of higher turnover number at high substrate concentration). In addition, Phe-167 of IEMT is shifted away from the binding pocket

compared with Phe-156 of EOMT1 and Phe-155 of CVOMT1, altering the geometry of the binding pocket (Figure 6). This could explain the broader substrate allowance for IEMT compared with CVOMT1 and may explain why this enzyme prefers substrates with propenyl side chains over those with allylic side chains.

Furthermore, as described previously, IEMT appears to have evolved recently from COMT in *C. breweri* (Wang and Pichersky, 1999). One of the major changes noted between these two enzymes is that a short sequence motif, MNQ, at residues 133 to 135 of COMT is changed to TAT in IEMT. This change was found to be responsible for the majority of the substrate discrimination observed between these two very closely related enzymes (Wang and Pichersky, 1999). When we evaluated the modeled IEMT (also based on the IOMT structure; Figure 6C), we found that the small aliphatic residue Ala-134 is located in the substrate binding pocket. The side chains of Thr-133 and Thr-135 appear to be directed away from the binding pocket. Significantly, the side chain of Ala-134 resides at the end of the binding pocket opposite where the catalytic His-273, Asp-274, and Glu-333 are located. In this position, Ala-134 is situated near the end of the phenylpropene side chain of the *t*-isoeugenol substrate, where it can stabilize hydrophobic moieties of potential substrates. In CVOMT1 and EOMT1, the residues that reside in this location in the active site also are small hydrophobic residues (Val-121 and Val-122 in CVOMT1 and Val-122 and Val-123 in EOMT1). These amino acid side chains would not interfere with the binding of alkene groups but would discriminate against hydrophilic group binding. If Ala-134 in IEMT were changed to the asparagine found in COMT, then the very hydrophilic side chain of the asparagine would be in close proximity to the very hydrophobic propenyl chain, destabilizing substrate binding. In COMT, however (or in the IEMT TAT→MNQ mutant, which uses caffeic acid as the preferred substrate [Wang and Pichersky, 1999]), this hydrophilic group could readily form hydrogen bonds to the oxygenated functionalities of the substrate, thereby stabilizing substrate binding.

Construction and Analysis of Mutated CVOMT1 and EOMT1 Enzymes

To determine the contribution to eugenol discrimination of Ser-261 in EOMT1 and of Phe-260 in CVOMT1, which was deduced from the modeling of their active sites, we changed the Ser-261 codon of *EOMT* into a phenylalanine codon (a single C-to-T mutation) and changed the Phe-260 codon of *CVOMT* into a serine codon (a single T-to-C mutation). *CVOMT1* and *EOMT1* constructs containing these modifications, *CVOMT1 F260S* and *EOMT1 S261F*, respectively, were inserted into the pCRT7/CT-TOPO TA expression vector, sequenced to verify that the correct modifications had been made and that no other modifications were introduced into the sequences, and expressed in *Escherichia coli*. The corresponding mutant recombinant proteins were assayed for substrate preference with chavicol, eugenol, *t*-isoeugenol, and caffeic acid (Figure 7). By comparing the activity of these mutants with the activity of the wild-type enzymes (Figure 5), two conclusions can be drawn. First, the CVOMT1 F260S mutant behaves like the native EOMT1 enzyme with regard to substrate preference. Instead of discriminating against eugenol, as the native protein does (Figure 5), the CVOMT1 F260S mutant uses eugenol much more efficiently than chavicol (Figure 7) and is able to catalyze the SAM-dependent *O*-methylation of *t*-isoeugenol with the same apparent efficiency as it did chavicol. In contrast, the mutant EOMT1 S261F functions like the native CVOMT1 enzyme. Instead of being able to use eugenol, *t*-isoeugenol, and chavicol, as the native enzyme does (Figure 5), the EOMT1 S261F mutant is able to effectively catalyze only the *O*-methylation of chavicol (Figure 7).

DISCUSSION

Basil glands express one OMT that is specific for chavicol and another OMT that has similar activity with chavicol but

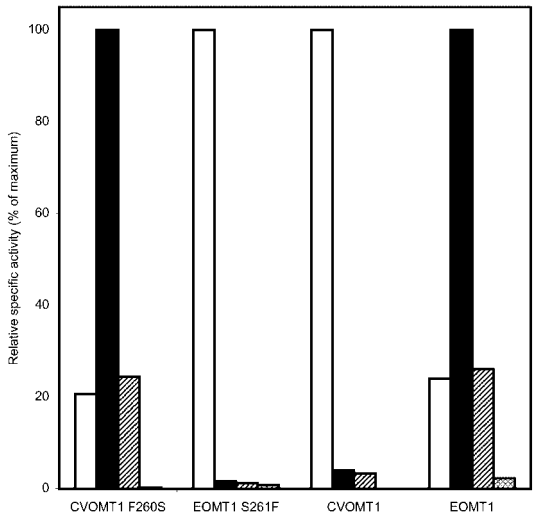

Figure 7. Substrate Specificity of Mutant Basil Phenylpropene OMTs.

The relative specific activities of mutant basil CVOMT1 (CVOMT1 F260S) and EOMT1 (EOMT1 S261F) are compared with the specific activities of the corresponding native enzymes (CVOMT1 and EOMT1, respectively) using key substrates: chavicol (white bars), eugenol (black bars), *t*-isoeugenol (diagonally hatched bars), and caffeic acid (cross-hatched bars). For each enzyme, the specific activity that is the highest is set as 100%.

has much higher activity with eugenol. Preliminary studies had demonstrated that the ratios of chavicol and eugenol OMT activities were not constant in sweet basil leaves (Wang, 1999; Lewinsohn et al., 2000; Gang et al., 2001). This could be explained by the presence of two separate OMT genes that were not always expressed at the same level or by the existence of some other factor that could modulate one or more of the OMT activities. If the observed differences were the result of two separate phenylpropene OMT enzymes, it was not clear whether the enzymes would have completely separate substrate preferences (i.e., each would be very specific for its substrate) or if the enzymes would overlap in substrate specificities. The cloning and heterologous expression of CVOMT and EOMT from sweet basil peltate glandular trichomes have answered these questions.

Two separate OMT gene types, which represent CVOMT and EOMT enzymes, were isolated from the peltate glandular trichomes of basil line EMX-1 leaves (Figure 3). RNA gel blot analysis demonstrated that the mRNA transcripts encoding these enzymes are highly expressed in the peltate glandular trichomes of the basil line (EMX-1) that produces large amounts of methylchavicol (and some methyleugenol as well) but are expressed at very low levels in a basil line (SW) that produces phenylpropenes that are not *para-O*-methylated (Figure 4). The mRNA transcript expression of phenylpropene OMTs (CVOMT and EOMT) followed the general pattern of glandular trichome development on basil leaves. As the leaves begin to develop, they produce the glandular trichomes. As these develop, the enzyme levels are high (as indicated by specific enzyme activity) and the mRNA transcript levels are high as well. There also are more glands per area in young leaves, before cell expansion (Gang et al., 2001). But as the glands reach maturity, the levels of OMT enzyme activity and mRNA transcripts decrease. These mRNA expression results supported enzyme assay results obtained previously (Wang, 1999; Lewinsohn et al., 2000; Gang et al., 2001). Quantitative RT-PCR established that ~90 to 95% of the OMT transcripts encoded CVOMT, whereas the rest encoded EOMT. Because the catalytic efficiency of EOMT1 is ~10-fold higher than the catalytic efficiency of CVOMT1, the relative proportions of the two transcript levels are consistent with the relative levels of enzymatic activity observed in the plant (Figure 4).

Characterization of the recombinant CVOMT1 and EOMT1 proteins demonstrated that CVOMT is specific for chavicol, whereas EOMT1 has similar levels of activity with chavicol as CVOMT but is much more active with eugenol as the substrate. These separate activities explain the differences in the ratios of CVOMT and EOMT enzyme activities described above.

The difference in apparent K_m values observed for both CVOMT1 and EOMT1, as outlined in Table 1, must be interpreted with caution because the two enzymes displayed significant substrate inhibition at >1 mM for their substrates. Thus, the activities of CVOMT1 and EOMT1 are much lower at chavicol concentrations of 5 mM than at 50 μM. This property was observed for eugenol and *t*-isoeugenol as substrates for both EOMT1 and CVOMT1 as well, but it was strongest with chavicol as the substrate. These enzymes probably use an ordered substrate binding mechanism in which SAM binds first followed by the phenylpropene substrate. Substrate inhibition probably occurs because *S*-adenosylhomocysteine (SAH) needs to be released before the next phenylpropene substrate molecule binds if a productive reaction complex is to form subsequently. At higher phenylpropene substrate concentrations, however, the SAH is not released before another substrate molecule binds, leading to an unproductive complex. This property is facilitated by tight binding of SAH in the active site, which probably binds almost as tightly as SAM (Zubieta et al., 2001), although this needs to be tested further.

It remains to be determined what the relative activities of a heterodimeric enzyme (with one EOMT subunit and one CVOMT subunit) with the two substrates would be, if such heterodimers are formed. With a different set of OMT enzymes, which are involved in alkaloid biosynthesis (Frick and Kutchan, 1999), such heterodimers—formed in a heterologous expression system—had novel substrate specificities. However, the apparent K_m values for the heterodimers were several orders of magnitude higher that those for native enzymes and endogenous substrates.

The fact that CVOMT1 has a lower catalytic efficiency for chavicol than EOMT1 has with eugenol should not lead to the conclusion that CVOMT is not capable of serving as a viable enzyme in the plant glandular trichome system. On the contrary, it is well established that enzymes involved in plant specialized metabolism often have low turnover numbers. To overcome this lower catalytic efficiency, plants often express such enzymes at very high levels in the appropriate tissue and cell type to achieve the required level of protein activity (White et al., 1998). It should be noted that EMX-1 basil produces >20-fold more methylchavicol than methyleugenol (Gang et al., 2001), but this could not be the result of differences in OMT activities (indeed, CVOMT and EOMT activities in EMX-1 glands are comparable). The cause of the difference in methylchavicol and methyleugenol production in EMX-1 must reside in differences in earlier steps of the pathways leading to chavicol and eugenol.

Evolution of Enzyme Specificity in the SMOMT Family

The crystal structures of IOMT and ChOMT were reported recently (Zubieta et al., 2001). In addition, the structure of COMT also has been solved (C. Zubieta and J.P. Noel, unpublished results), and this was found to be very similar to the structures of IOMT and ChOMT. These structures revealed that the active sites of these enzymes are very similar in general structure. The central region of the active site is lined with aromatic and aliphatic amino acid residues whose positions and orientation appear to be responsible for producing the specific geometry that determines the level of substrate discrimination that occurs with each enzyme. For

example, the side chains of Asn-310 and Cys-313 of IOMT were found to be localized in the central region of the binding pocket, and these were found to stabilize, via hydrogen bonds, the hydroxyl group of the proposed in vivo substrate of IOMT (Zubieta et al., 2001).

Molecular modeling of the CVOMT1 and EOMT1 amino acid sequences, based on the IOMT and COMT crystal structures, gave a rational explanation for the differences in substrate preference of these two closely related enzymes. A different amino acid in a single position in the active site (Phe-260 in CVOMT1 and the equivalent Ser-261 in EOMT1) appeared to be responsible for the difference in substrate specificity between EOMT and CVOMT (Figures 6A and 6B). This explanation was tested empirically and shown to be correct (Figure 7). In addition, the results of modeling of *C. breweri* IEMT also explain how the change of a single amino acid in the progenitor COMT protein, changing Asn-134 to an alanine, also was sufficient to create a new enzyme (Wang and Pichersky, 1999) (Figure 6C).

The basil phenylpropene OMTs clearly evolved their substrate specificity independently of the analogous enzyme in *C. breweri*. This represents another example of the specialized type of convergent evolution termed repeated evolution (Cseke et al., 1998; Pichersky and Gang, 2000). And although the evolution of basic phenylpropene OMT activity in these two lineages may not be very recent, it is clear that more recent changes in enzyme specificity have occurred in the basil lineage. However, it is not clear if CVOMT evolved from EOMT or vice versa, and an analysis of related enzymes in related species may be required to answer this question. If CVOMT evolved from EOMT, then CVOMT evolution is a case of an enzyme evolving an increased substrate specificity and not a new substrate specificity. If the direction was from CVOMT to EOMT, then this truly is a case of a new enzyme (i.e., with a new substrate specificity) that possibly originated very recently. Regardless of the actual direction of evolution in this case, these results clearly show that a single amino acid substitution may be all that is required to produce a new SMOMT enzyme involved in plant specialized (secondary) metabolite biosynthesis. A similar difference in substrate specificity attributable to a single amino acid difference was reported by Frick and Kutchan (1999), although the actual in vivo substrates of the two OMTs in that study were not clear. These results suggest that new enzymes in plant specialized metabolite biosynthesis (secondary metabolism) with new catalytic functions may arise rapidly or instantaneously. Furthermore, because the evolution of new OMTs with new substrate specificities is relatively simple, it is not surprising that OMTs with similar substrate specificities evolved independently in different plant lineages more than once.

Because of the great importance that such enzymes play in determining the defensive capabilities of the plant, in which new modifications of existing specialized compounds need to occur quickly in response to new pathogens or herbivores or to the development of resistance in a present pest, or to attract new pollinators, rapid evolution in the enzymes involved may be the norm. Both gene duplication and divergence and the faster route of divergence among alleles of loci encoding enzymes in plant specialized metabolite biosynthesis (Pichersky and Gang, 2000) may be the means by which plants are able to respond to the continually changing environment in which they grow.

METHODS

Plant Material

Basil (*Ocimum basilicum*) lines EMX-1 and SW were grown under controlled conditions as described previously (Gang et al., 2001).

Chemicals and Radiochemicals

^{3}H-Methyl-*S*-adenosyl-L-methionine (15 Ci/mmol) and ^{14}C-methyl-*S*-adenosyl-L-methionine (55 mCi/mmol) were obtained from Amersham. *S*-Adenosyl-L-methionine and all other chemicals were purchased from Sigma Chemical Co. (St. Louis, MO), except the CoA esters, which were synthesized in the laboratory (see below).

Synthesis of CoA Esters

CoA esters of several hydroxycinnamic acids were synthesized using a modified imidazolide method (Pabsch et al., 1991). Imidazolides of the corresponding acids were prepared as described previously (Pabsch et al., 1991). The reaction was monitored for purity and completion by thin-layer chromatography (silica gel; solvent: diethylether acidified with 1% acetic acid and visualized under UV light). Acid imidazolides were used in twofold excess compared with the CoA sodium salt (Sigma). The reaction was monitored as described above with a solvent system of *n*-butanol:acetic acid:water (63:10:27). CoA esters were identified with a delayed nitroprusside reaction (Stadtman, 1957). The reaction was terminated by extraction (three times) with ethyl acetate (phase separation achieved by centrifugation). After evaporation of the organic solvent, ammonium acetate was added to the water phase to a final concentration of 2% and the mixture was loaded onto a preconditioned 1000-mg SPE cartridge (Chromabond C-18 ec; Machery-Nagel, Duren, Germany); conditioning involved consecutive washes with methanol, dH_2O, and 2% ammonium acetate solution (five column volumes each). The column was washed with 2% ammonium acetate solution until the flowthrough showed the absence of free CoA (determined with a spectrophotometer). The CoA esters were recovered by elution with distilled water. Fractions containing the CoA esters were identified using a spectrophotometer and lyophilized overnight. HPLC analysis showed a purity of >90% (Nova-Pak RP-C18, 3.9 × 300 mm; Waters, Milford, MA). Flow was 1 mL/min in solvent A (acetonitrile) and solvent B (20 mM KH_2PO_4, pH 2.9). The gradient was 5% A in B for 0 to 5 min, 5 to 38% A in B for min 5 to 32, 38 to 75% A in B for min 32 to 35, 75 to 5% A in B for min 35 to 40, and 5% A in B for min 40 to 45. CoA esters were stored lyophilized or in solution at pH 6.0 for several months at –80°C without noticeable degradation.

Cloning of Basil *O*-Methyltransferases

A cDNA for basil caffeic acid *O*-methyltransferase (*COMT*1) was isolated previously (Wang et al., 1999). An expressed sequence tag (EST) database was constructed previously by sequencing random clones from a basil peltate glandular trichome cDNA library (Gang et al., 2001). These ESTs are available for searching upon request. Two types of closely related *O*-methyltransferase (OMT) genes were identified in the EST database, although all sequences were incomplete. Rapid amplification of cDNA ends (Chenchik et al., 1996; Matz et al., 1999) and genome walking (Siebert et al., 1995) were used independently to obtain the sequence missing from the 5′ end of the genes. Because the 5′ and 3′ ends of the genes were identical (the differences were found in the middle of the coding region), two specific primers were designed (5′ primer, 5′-AATGGCATTGCAAAAAGTA-3′; 3′ primer, 5′-GATAGCTACAATTTTAAGG-3′) and used in reverse transcriptase–mediated polymerase chain reaction (RT-PCR) with the basil peltate glandular trichome first-strand cDNA to obtain complete coding regions. Two unique genes (*CVOMT*1 for chavicol OMT and *EOMT*1 for eugenol OMT) were amplified and transferred into the pCRT7/CT-TOPO TA expression vector (Invitrogen). After complete sequencing, the resulting constructs were transformed into *Escherichia coli* BL21(DE3)pLysS cells for expression.

Sequence Analysis

Amino acid sequence alignments and neighbor-joining trees were generated using the ClustalX computer program (Thompson et al., 1997). The resulting dendrograms were visualized using the NJplot computer program (Perrière and Gouy, 1996).

RNA Gel Blot Analysis

Total RNAs from isolated peltate glandular trichomes and from whole leaf tissue from basil lines EMX-1 and SW were purified as described previously (Gang et al., 2001). A ^{32}P-labeled probe for *CVOMT*1 was constructed using the *Redi*prime II Kit (Amersham Pharmacia Biotech) from a gel-purified PCR product (~500 bp) amplified using primers designed from the *CVOMT*1 cDNA sequence (*CVOMT*1 5′ probe primer, 5′-TTTCCCAATTACTCAAGGCC-3′; *CVOMT*1 3′ probe primer, 5′-CCCTCCAACGCCAACTGC-3′). Formaldehyde agarose (1%) gel electrophoresis, RNA gel blot analysis, probe hybridization at 65°C, and washes were performed under standard conditions (Sambrook et al., 1989) using Hybond-XL nylon membranes (Amersham Pharmacia Biotech) and 4 × SSC (1 × SSC is 0.15 M NaCl and 0.015 M sodium citrate) as the hybridization buffer.

Quantitative RT-PCR

Total RNAs, isolated as for RNA gel blot analysis, from 0.5-, 1-, and 3-cm leaves as well as from peltate glands were used with the First-Strand cDNA Synthesis Kit (Amersham Pharmacia Biotech) to produce first-strand cDNAs. Gene-specific primer pairs were designed that amplified only the gene of interest when control PCR procedures were performed; these reactions used plasmids containing either *CVOMT*1 or *EOMT*1 as a template. The primer pairs were *CVOMT*1 5′ probe primer with *CVOMT*1 3′ probe primer and *EOMT*1 5′ probe primer (5′-TTTCCCAGTTACTCCAATCT-3′) with *EOMT*1 3′ probe primer (5′-CCCTTCCATAACGACCGT-3′). Several amplification cycle numbers were tested for each cDNA sample. The optimal number of cycles, which produced faint yet clearly detectable bands for the *CVOMT*1 gene products, was determined to be 23 cycles for 1-cm leaf and peltate gland cDNAs and 26 cycles for 0.5- and 3-cm leaf cDNAs. These cycle numbers were used for templates with *CVOMT*1 and *EOMT*1 primer sets in triplicate 50-μL PCR procedures. An identical number of cycles was used for both *CVOMT*1 and *EOMT*1 for each leaf cDNA sample. Slot blotting and DNA gels followed by DNA gel blotting were then performed in duplicate with 10 μL of each sample. Hybond N^+ nylon membrane (Amersham Pharmacia Biotech) was used for both applications. The resulting blot pairs then were prehybridized and hybridized (according to the manufacturer's instructions) to either *CVOMT*1- or *EOMT*1-labeled probe, produced from PCR products (using the appropriate primer pair with the corresponding plasmid templates), which were labeled using the *Redi*prime II kit (Amersham Pharmacia Biotech). After overnight incubation at 65°C, the blots were washed according to the membrane manufacturer's instructions. After overnight exposure to a phosphorimager screen (Bio-Rad Laboratories), the relative signal intensity for each sample was measured using the Molecular Imager software package (Bio-Rad Laboratories). DNA gel blots and slot blots gave comparable results.

Preparation of Crude Cell-Free Extracts from *E. coli*

Single isolated bacterial colonies from freshly streaked plates (grown on Luria-Bertani agar medium containing 50 μg/mL ampicillin and 15 μg/mL chloramphenicol) were used to inoculate 2-mL liquid cultures (in Luria-Bertani medium with 50 μg/mL ampicillin), which were grown overnight at 37°C. An aliquot (500 μL) of these cultures was used to inoculate 50-mL liquid cultures. Once the cultures reached a cell density of 0.3 to 0.6 OD_{600}, recombinant protein expression was induced by the addition of 0.3 mM isopropylthio-β-galactoside. After overnight incubation at room temperature, the cells were pelleted by centrifugation at 20,000*g* for 10 min at 4°C. The pellets were stored at −20°C. Cells containing expressed recombinant protein were resuspended in 500 μL of 50 mM bis-Tris, pH 7.0, containing 10% glycerol, 14 mM 2-mercaptoethanol, 1 mM EDTA, and 10 mM NaCl. After the cells were lysed by adding lysozyme to a final concentration of 1 μg/mL, incubating the resulting mixture on ice for 20 min, and freezing (in liquid N_2) and thawing two times, cellular debris were removed by centrifugation at 20,000*g* for 10 min at 4°C. This crude bacterial lysate was used for further purification steps and enzymatic assays.

Partial Enzyme Purification

All procedures were performed at 0 to 4°C using buffer A (50 mM bis-Tris, pH 7.0, containing 10% glycerol, 5 mM $Na_2S_2O_5$, 10 mM 2-mercaptoethanol, and 1 mM EDTA). Protein concentrations were measured according to Bradford (1976) using the Bio-Rad protein reagent with BSA (Sigma) as a standard.

Gel Filtration

The crude bacterial lysate (3 mL) was applied to a Bio-Gel P-6 column (Bio-Rad, Hercules, CA; 1 × 10 cm) and preequilibrated in buffer A, and proteins were eluted in the same buffer. Eluting fractions containing enzyme activity were combined.

Ion Exchange Chromatography

The pooled fractions (~2 mL) were applied to a Hitrap Q Sepharose column (1 × 5 cm; Amersham Pharmacia Biotech) equilibrated with buffer A. The flow rate was 1 mL/min. Buffer B was the same as buffer A but contained 1 M KCl. Proteins were eluted from the column with the following gradient program: 10 mL of 0% buffer B, 40 mL of 0 to 60% buffer B, and 10 mL of 100% buffer B. Fractions were tested for enzyme activity, and active fractions were combined.

Subunit and Native Molecular Mass

The subunit molecular mass of each enzyme was determined by SDS-PAGE (12% polyacrylamide), and the molecular mass of the native enzymes was estimated using gel filtration chromatography through a Superdex 75 Hiload Prep 16/60 column (Amersham Pharmacia Biotech). Molecular mass standards were alcohol dehydrogenase (150 kD), phosphorylase *b* (97 kD), BSA (66 kD), carbonic anhydrase (29 kD), cytochrome *c* (12.4 kD), and aprotinin (6.5 kD), all from Sigma.

Enzyme Assays

The standard radiochemical assay mixture for the recombinant proteins consisted of 70 μL of buffer A, 10 μL of enzyme solution (1.5 to 3 μg of protein), 10 μL of substrate solution (in ethanol; final concentration of substrates was 1 mM for COMT and 0.1 mM for CVOMT and EOMT), and 10 μL of ^{3}H-*S*-adenosylmethionine (SAM) (20,000 cpm per reaction; final concentration of substrates was 180 μM for COMT and 15 μM for CVOMT and EOMT) in a total volume of 100 μL. After incubation at 30°C for 0.5 hr, the reactions were stopped by the addition of 10 μL of 2 N HCl. Radiolabeled products then were extracted by the addition of 1 mL of ethyl acetate followed by vortexing. After centrifugation (1 min at 20,000*g*) to separate the phases, 800 μL of the upper (ethyl acetate) phase was used for scintillation counting (3 mL of scintillation fluid—4 g/L 2,5-diphenyloxazol and 0.05 g/L 2,2′-*p*-phenylene-bis[5-phenyloxazol] in toluene—in a liquid scintillation counter). Verification of assay product identity was achieved by performing assays as described above but using nonradiolabeled SAM as cofactor and concentrating the ethyl acetate–extracted products under dry nitrogen. The concentrated products then were resuspended in an appropriate solvent and analyzed by gas chromatography–mass spectrometry (GC-MS) or liquid chromatography–mass spectrometry (LC-MS).

GC-MS Analysis

Volatile compounds were analyzed with a Hewlett-Packard GC-MS system (Palo Alto, CA) equipped with an HP-5 [30 m × 0.25 mm] fused silica capillary column. Helium (1 mL/min) was used as a carrier gas. The injector was set for splitless injection at 250°C, and the detector was set at 280°C. The oven was set to 50°C for 1 min after injection, and then the temperature was increased to 200°C at a rate of 4°C/min. The mass-to-charge ratio was 45 to 450, with an energy of 70 electron volts. Eluting compounds were identified using a GC-MS library and by comparison of mass spectra and retention times with authentic samples.

LC-MS Analysis

Nonvolatile compounds were analyzed on a Micromass Quattro LCZ triple-quadropole mass spectrometer (Micromass, Beverly, MA) attached to a Waters 2690 Separations Module with attached column oven. HPLC separation of the compounds over a Waters Nova-Pak C_{18} column (4.6 mm × 30 cm) was achieved using a 30-min linear gradient from 5% acetonitrile in 0.05% formic acid to 100% acetonitrile, with the flow rate set at 1 mL/min and the column temperature set to 40°C. In-line UV light spectra (200 to 600 nm) were obtained using an attached Waters 996 photodiode array detector. Splitting before entrance into the mass spectrometer reduced the flow rate to 100 μL/min. Electrospray ionization in the Micromass Z-Spray source was achieved in negative ion mode by setting the capillary voltage to 2.5 to 3.0 kV and setting the cone voltage to between 30 and 80 V depending on the compound to be analyzed. The desolvation gas flow rate and temperature were set to 270 L/hr and 250°C, respectively, and the source temperature was set to 140°C. Other source parameters were set to standard conditions recommended by Micromass. Eluting compounds were identified by comparison of UV light spectra, mass spectra, and elution volume with authentic samples (analyzed on the same instrument with identical HPLC elution and source parameters).

Kinetic Properties

Standard methods (e.g., using Lineweaver-Burk, Eddie-Hofstee, and Michaelis-Menten equations [Segel, 1993]) were used to determine apparent K_m and V_{max} for CVOMT, EOMT, and COMT from basil using modified standard radiochemical assays. For apparent K_m with SAM, the concentration of substrate (chavicol for CVOMT, eugenol for EOMT, and caffeic acid for COMT) was kept constant at 0.1, 0.1, and 1 mM, respectively, whereas the concentration of SAM was varied. For apparent K_m with various substrates, SAM concentration was kept constant at 180 μM for COMT and 15 μM for CVOMT and EOMT, whereas the concentrations of the other substrates were varied.

Molecular Modeling

The sequences for CVOMT, EOMT, and (iso)eugenol OMT were fit to the three-dimensional structure obtained for isoflavone OMT using Modeller (Sali and Blundell, 1993). The resulting pdb files were visualized using Swiss PDB Viewer (Guex and Peitsch, 1997), and three-dimensional stereo images were drawn using POV-Ray (X-POV-Team, 1997).

Construction of Mutant OMT Enzymes

Ser-261 in EOMT was mutated to a phenylalanine residue and Phe-260 in CVOMT was mutated to a serine residue via the DNA PCR method (Ho et al., 1989) using *Taq* DNA polymerase (Fisher Scientific). The external primers were CVOMT-Nt1 (5′-AATGGCATTGCAAAATATG-3′) and OMT-Ct1 (5′-TTTTAAGGATAAGCCTCTA-3′) for CVOMT1 and EOMT-Nt1 (5′-AATGGCATTGCAAAAAGTA-3′) and OMT-Ct1 (5′-TTTTAAGGATAAGCCTCTA-3′) for EOMT1. One set of complementary mutating primers was designed for each gene: CVOMT1-F1 (5′-CTTCTCAAG***TCT***ATAATACACGA-3′) and CVOMT1-R1 (5′-TCGTGTATTAT***AG***ACTTGAGAAG-3′) for CVOMT1 and EOMT1-F1 (5′-CTTCTAAAG***TT***TATAATACATGA-3′) and EOMT1-R1 (5′-TCATGTATTAT***AA***ACTTTAGAAG-3′) for EOMT1. Bases coding for the mutated

amino acid are shown in italics, and bases causing the mutation are shown in boldface.

Accession Numbers

The accession numbers for the proteins listed in Figure 2 are AAD24001 (*Pinus radiata* COMT), AAC49708 (*Pinus taeda* COMT), AAB71141 (*Clarkia breweri* COMT), AAC01533 (*C. breweri* IEMT), CAA52814 (*Eucalyptus gunnii* COMT), AAB46623 (*Medicago sativa* COMT), CAA01820 (*Populus balsamifera* COMT), CAA58218 (*Prunus dulcis* COMT), AAB96879 (*Arabidopsis thaliana* COMT1), AAA86982 (*Chrysosplenium americanum* COMT), AAD38189 (*Ocimum basilicum* COMT1), S36403 (*Nicotiana tabacum* COMT), T12259 (*Capsicum annuum* OMT), AAA86718 (*Zinnia elegans* COMT), AAB48059 (*M. sativa* ChOMT), T04963 (*A. thaliana* OMT), S52015 (*Hordeum vulgare* F7OMT), P47917 (*Zea mays* OMT), AAD10485 (*Triticum aestivum* OMT), T06786 (*Pisum sativum* HMOMT), T09299 (*M. sativa* OMT), T09254 (*M. sativa* IOMT), AF435007 (*O. basilicum* CVOMT1), AF435008 (*O. basilicum* EOMT1), BAA86059 (*Pyrus pyrifolia* OMT), CAA11131 (*P. dulcis* OMT), and AAB71213 (*Prunus armeniaca* OMT).

ACKNOWLEDGMENTS

This research was supported in part by a competitive grant from the United States Department of Agriculture National Research Initiative (Grant No. 0003497). T.B. was supported in part by a Deutscher Akademischer Austausch Dienst fellowship (Gemeinsames Hochschulsonderprogramm III von Bund und Ländern, Germany).

Received August 2, 2001; accepted November 1, 2001.

REFERENCES

Adams, S., and Weidenborner, M. (1996). Mycelial deformations of *Cladosporium herbarum* due to the application of eugenol or carvacrol. J. Essential Oil Res. **8,** 535–540.

Bradford, M.M. (1976). A rapid and sensitive method for the quantitation of microgram quantities of protein utilizing the principle of protein-dye binding. Anal. Biochem. **72,** 248–254.

Chatterjee, A., Sukul, N., Laskar, S., and Ghoshmajumdar, S. (1982). Nematicidal principles from two species of Lamiaceae, *Ocimum sanctum* and *Ocimum basilicum*. J. Nematol. **14,** 118–122.

Chenchik, A., Zhu, Y., Diatchenko, L., Li, R., Hill, J., and Siebert, P. (1996). Generation and use of high-quality cDNA from small amounts of total RNA by SMART PCR. In RT-PCR Methods for Gene Cloning and Analysis, P. Siebert and J. Larrick, eds (Westborough, MA: BioTechniques Books), pp. 305–319.

Collendavelloo, J., Legrand, M., Geoffroy, P., Barthelemy, J., and Fritig, B. (1981). Purification and properties of the three *o*-diphenol-*O*-methyltransferases of tobacco leaves. Phytochemistry **20,** 611–616.

Cseke, L., Dudareva, N., and Pichersky, E. (1998). Structure and evolution of linalool synthase. Mol. Biol. Evol. **15,** 1491–1498.

Frick, S., and Kutchan, T.M. (1999). Molecular cloning and functional expression of *O*-methyltransferases common to isoquinoline alkaloid and phenylpropanoid biosynthesis. Plant J. **17,** 329–339.

Gang, D.R., Wang, J., Dudareva, N., Nam, K.H., Simon, J., Lewinsohn, E., and Pichersky, E. (2001). An investigation of the storage and biosynthesis of phenylpropenes in sweet basil (*Ocimum basilicum* L.). Plant Physiol. **125,** 539–555.

Gildemeister, E., and Hoffmann, F.R. (1913). Ätherischen Öle. (Milwaukee, WI: Pharmaceutical Review Publishing Co.).

Grossman, J. (1993). Botanical pesticides in Africa. Int. Pest Manag. Pract. **15,** 1–9.

Guenther, E. (1949). The Essential Oils. (Princeton, NJ: D. Van Nostrand Co., Inc.).

Guex, N., and Peitsch, M.C. (1997). SWISS-MODEL and the Swiss-PdbViewer: An environment for comparative protein modeling. Electrophoresis **18,** 2714–2723.

Guo, D.J., Chen, F., Inoue, K., Blount, J.W., and Dixon, R.A. (2001). Downregulation of caffeic acid 3-*O*-methyltransferase and caffeoyl CoA 3-*O*-methyltransferase in transgenic alfalfa: Impacts on lignin structure and implications for the biosynthesis of G and S lignin. Plant Cell **13,** 73–88.

He, X.-Z., Reddy, J.T., and Dixon, R.A. (1998). Stress responses in alfalfa (*Medicago sativa* L.). XXII. cDNA cloning and characterization of an elicitor-inducible isoflavone 7-*O*-methyltransferase. Plant Mol. Biol. **36,** 43–54.

Ho, S.N., Hunt, H.D., Horton, R.M., Pullen, J.K., and Pease, L.R. (1989). Site-directed mutagenesis by overlap extension using the polymerase chain reaction. Gene **77,** 51–59.

Ibrahim, R.K., Bruneau, A., and Bantignies, B. (1998). Plant *O*-methyltransferases: Molecular analysis, common signature and classification. Plant Mol. Biol. **36,** 1–10.

Karapinar, M., and Aktug, S. (1987). Inhibition of foodborne pathogens by thymol, eugenol, menthol and anethole. Int. J. Food Microbiol. **4,** 161–166.

Klischies, M., Stockigt, J., and Zenk, M.H. (1975). Biosynthesis of the allylphenols eugenol and methyleugenol in *Ocimum basilicum* L. Chem. Commun. **21,** 879–880.

Lawrence, B.M. (1992). Chemical components of labiate oils and their exploitation. In Advances in Labiate Science, R.M. Harley and T. Reynolds, eds (Kew, UK: Royal Botanical Gardens).

Lewinsohn, E., Ziv-Raz, I., Dudai, N., Tadmor, Y., Lastochkin, E., Larkov, O., Chaimovitsh, D., Ravid, U., Putievsky, E., Pichersky, E., and Shoham, Y. (2000). Biosynthesis of estragole and methyleugenol in sweet basil (*Ocimum basilicum* L): Developmental and chemotypic association of allylphenol *O*-methyltransferase activities. Plant Sci. **160,** 27–35.

Manitto, P., Monti, D., and Gramatica, P. (1974). Biosynthesis of phenylpropanoid compounds. I. Biosynthesis of eugenol in *Ocimum basilicum* L. J. Chem. Soc. Perkin Trans. I **14,** 1727–1731.

Manitto, P., Gramatica, P., and Monti, D. (1975). Biosynthesis of phenylpropanoid compounds. II. Incorporation of specifically labelled cinnamic acids into eugenol in basil [*Ocimum basilicum*]. J. Chem. Soc. Perkin Trans. I **16,** 1549–1551.

Martz, F., Maury, S., Pincon, G., and Legrand, M. (1998). cDNA cloning, substrate specificity and expression study of tobacco caffeoyl-CoA 3-*O*-methyltransferase, a lignin biosynthetic enzyme. Plant Mol. Biol. **36,** 427–437.

Matz, M., Lukyanov, S., Bogdanova, E., Diatchenko, L., and Chenchik, A. (1999). Amplification of cDNA ends based on template-switching effect and step-out PCR. Nucleic Acids Res. **27,** 1558–1560.

Maury, S., Geoffroy, P., and Legrand, M. (1999). Tobacco *O*-methyltransferases involved in phenylpropanoid metabolism: The different caffeoyl-coenzyme A/5-hydroxyferuloyl-coenzyme A 3/5-*O*-methyltransferase and caffeic acid/5-hydroxyferulic acid 3/5-*O*-methyltransferase classes have distinct substrate specificities and expression patterns. Plant Physiol. **121,** 215–223.

Maxwell, C.A., Edwards, R., and Dixon, R.A. (1992). Identification, purification, and characterization of *S*-adenosyl-L-methionine-isoliquiritigenin 2′-*O*-methyltransferase from alfalfa (*Medicago sativa* L). Arch. Biochem. Biophys. **293,** 158–166.

Maxwell, C.A., Harrison, M.J., and Dixon, R.A. (1993). Molecular characterization and expression of alfalfa isoliquiritigenin 2′-*O*-methyltransferase, an enzyme specifically involved in the biosynthesis of an inducer of *Rhizobium meliloti* nodulation genes. Plant J. **4,** 971–981.

Mbeguie-A-Mbeguie, D., Gomez, R.-M., and Fils-Lycaon, B. (1997). Sequence of an *O*-methyltransferase from apricot fruit (accession no. U82011): Gene expression during fruit ripening (PGR97–118). Plant Physiol. **114,** 1569.

Miyao, S. (1975). Inhibitory effects of ethanol extract of mace and eugenol on the growth of microorganisms isolated from Vienna sausages. Nihon Shokuhin Eisei Gakkai **16,** 412–416.

Obeng-Ofori, D., and Reichmuth, C. (1997). Bioactivity of eugenol, a major component of essential oil of *Ocimum suave* (Wild.) against four species of stored-product Coleoptera. Int. J. Pest Manage. **43,** 89–94.

Pabsch, K., Petersen, M., Rao, N.N., Alfermann, A.W., and Wandrey, C. (1991). Chemo-enzymatic synthesis of rosmarinic acid. Rec. Trav. Chim. Pays-Bas **110,** 199–205.

Parvathi, K., Chen, F., Guo, D.J., Blount, J.W., and Dixon, R.A. (2001). Substrate preferences of *O*-methyltransferases in alfalfa suggest new pathways for 3-*O*-methylation of monolignols. Plant J. **25,** 193–202.

Pellegrini, L., Geoffroy, P., Fritig, B., and Legrand, M. (1993). Molecular cloning and expression of a new class of ortho-diphenol-*O*-methyltransferases induced in tobacco (*Nicotiana tabacum* L.) leaves by infection or elicitor treatment. Plant Physiol. **103,** 509–517.

Perrière, G., and Gouy, M. (1996). WWW-Query: An on-line retrieval system for biological sequence banks. Biochimie **78,** 364–369.

Pichersky, E., and Gang, D.R. (2000). Genetics and biochemistry of secondary metabolites in plants: An evolutionary perspective. Trends Plant Sci. **5,** 439–445.

Sali, A., and Blundell, T.L. (1993). Comparative protein modelling by satisfaction of spatial restraints. J. Mol. Biol. **234,** 779–815.

Sambrook, J., Fritsch, E.F., and Maniatis, T. (1989). Molecular Cloning: A Laboratory Manual, 2nd ed. (Cold Spring Harbor, NY: Cold Spring Harbor Laboratory Press).

Sangwan, N., Verman, B., Verma, K., and Dhindsa, K. (1990). Nematicidal activity of some essential plant oils. Pestic. Sci. **28,** 331–335.

Schmitt, D., Pakusch, A.E., and Matern, U. (1991). Molecular-cloning, induction, and taxonomic distribution of caffeoyl-CoA 3-*O*-methyltransferase, an enzyme involved in disease resistance. J. Biol. Chem. **266,** 17416–17423.

Segel, I.H. (1993). Enzyme Kinetics: Behavior and Analysis of Rapid Equilibrium and Steady-State Enzyme Systems. (New York: John Wiley and Sons).

Senanayake, U.M., Wills, R.B.H., and Lee, T.H. (1977). Biosynthesis of eugenol and cinnamic aldehyde in *Cinnamomum zeylanicum*. Phytochemistry **16,** 2032–2033.

Shukla, R., and Prasad, V. (1985). Population fluctuations of the oriental fruit fly, *Dacus dorsalis* Hendel, in relation to hosts and abiotic factors. Trop. Pest Manage. **31,** 273–275.

Siebert, P.D., Chenchik, A., Kellogg, D.E., Lukyanov, K.A., and Lukyanov, S.A. (1995). An improved method for walking in uncloned genomic DNA. Nucleic Acids Res. **23,** 1087–1088.

Sisk, C., Shorey, H., Gerber, R., and Gaston, L. (1996). Semiochemicals that disrupt foraging by the Argentine ant (Hymenoptera: Formicidae): Laboratory bioassays. J. Econ. Entomol. **89,** 381–385.

Stadtman, E.R. (1957). Preparation and Assay of Acyl Coenzyme A and Other Thiol Esters: Use of Hydroxylamine. Methods Enzymol. **III**, 931–941.

Suelves, M., and Puigdomenech, P. (1998). Specific mRNA accumulation of a gene coding for an *O*-methyltransferase in almond (*Prunus amygdalus*, Batsch) flower tissues. Plant Sci. **134,** 79–88.

Thompson, J.D., Gibson, T.J., Plewniak, F., Jeanmougin, F., and Higgins, D.G. (1997). The ClustalX Windows interface: Flexible strategies for multiple sequence alignment aided by quality analysis tools. Nucleic Acids Res. **24,** 4876–4882.

Vander Mijnsbrugge, K., Meyermans, H., Van Montagu, M., Bauw, G., and Boerjan, W. (2000). Wood formation in poplar: Identification, characterization, and seasonal variation of xylem proteins. Planta **210,** 589–598.

Wang, J. (1999). Molecular Characterization of an *O*-Methyltransferase Involved in Floral Scent Production in *Clarkia breweri*. Ph.D. Dissertation. (Ann Arbor, MI: University of Michigan).

Wang, J., and Pichersky, E. (1998). Characterization of *S*-adenosyl-L-methionine:(iso)eugenol *O*-methyltransferase involved in scent production in *Clarkia breweri*. Arch. Biochem. Biophys. **349,** 153–160.

Wang, J., and Pichersky, E. (1999). Identification of specific residues involved in substrate discrimination in two plant *O*-methyltransferases. Arch. Biochem. Biophys. **368,** 172–180.

Wang, J., Dudareva, N., Kish, C.M., Simon, J.E., Lewinsohn, E., and Pichersky, E. (1999). Nucleotide sequences of two cDNAs encoding caffeic acid *O*-methyltransferases from sweet basil (*Ocimum basilicum*). Plant Physiol. **120,** 1205.

White, W.L.B., Arias-Garzon, D.I., McMahon, J.M., and Sayre, R.T. (1998). Cyanogenesis in cassava: The role of hydroxynitrile lyase in root cyanide production. Plant Physiol. **116,** 1219–1225.

Wu, Q., Preisig, C.L., and VanEtten, H.D. (1997). Isolation of the cDNAs encoding (+)-6a-hydroxymaackiain 3-*O*-methyltransferase, the terminal step for the synthesis of the phytoalexin pisatin in *Pisum sativum*. Plant Mol. Biol. **35,** 551–560.

X-POV-Team. (1997). POV-Ray: Persistence of vision ray-tracer. Available at http://www.povray.org.

Ye, Z.-H., and Varner, J. (1995). Differential expression of two *O*-methyltransferases in lignin biosynthesis in *Zinnia elegans*. Plant Physiol. **108,** 459–467.

Zubieta, C., He, X.-Z., Dixon, R.A., and Noel, J.P. (2001). Structures of two natural product methyltransferases reveal the basis for substrate specificity in plant *O*-methyltransferases. Nat. Struct. Biol. **8,** 271–279.